Large excitonic effects in group-IV sulfide monolayers

Blair R. Tuttle,[1,2] Saeed M. Alhassan,[3] and Sokrates T. Pantelides[1,4]
[1]*Department of Physics and Astronomy, Vanderbilt University, Nashville, Tennessee 37235, USA*
[2]*Department of Physics, Penn State Behrend, Erie, Pennsylvania 16563, USA*
[3]*Department of Chemical Engineering, The Petroleum Institute, P.O. Box 2533, Abu Dhabi, United Arab Emirates*
[4]*Oak Ridge National Laboratory, Oak Ridge, Tennessee 37831, USA*
(Received 18 June 2015; revised manuscript received 30 September 2015; published 3 December 2015)

Large exciton binding energies are a distinguishing feature of two-dimensional semiconductors because of reduced screening, potentially leading to unique optoelectronic applications. Here we use electronic structure methods to calculate the properties of a two-dimensional material class: group-IV monosulfides including SiS, GeS, and SnS. Bulk SiS is predicted to be a metastable layered material. Quasiparticle excitations are calculated with the G_0W_0 method and the Bethe-Salpeter equation is are used to include electron-hole interactions. For monolayers, strongly bound excitons are found below the quasiparticle absorption edge. The predicted excitonic binding energies are as high as 0.7 eV. Due to large excitonic effects, these group-IV sulfide monolayers have great potential for nanoscale optoelectronic applications.

DOI: 10.1103/PhysRevB.92.235405 PACS number(s): 71.15.Mb, 71.20.Nr, 78.20.Ci, 71.35.−y

I. INTRODUCTION

Since the discovery of graphene, there has been tremendous interest in the discovery of two-dimensional (2D) materials with unusual properties [1–4]. Two-dimensional materials with semiconducting properties, such as MoS_2 and phosphorene, are particularly interesting from both a basic [5–7] and applied [3,5,8] research perspective. Semiconducting two-dimensional materials are promising for electronic, optical, and other applications. Even though their bonding is not strictly planar, both MoS_2 and phosphorene are considered two-dimensional materials because their structure involves a single monolayer of a multilayered bulk system. The electronic structure of monolayers differs both quantitatively and qualitatively from their bulk counterparts. For instance, monolayer MoS_2 has a direct wide band gap ($E_g \sim 2.7$ eV), whereas bulk MoS_2 has a relatively small and indirect gap, $E_g \sim 1.3$ eV [9].

Quantum confinement effects in monolayer semiconductors result in novel electronic properties including strongly bound excitons, which dominate the optoelectronic response of these systems [2]. Due to these large excitonic effects, new basic and applied physics phenomena can be investigated. For instance, in MoS_2 monolayers, the deepest exciton exhibits non-Rydberg excited states [7]. Also, the direct excitonic gap in MoS_2 allows for the construction of optoelectronic devices such as 2D optical sensors and emitters [10]. Finding new monolayered materials with strongly bound excitons would enhance our understanding of exciton physics and open opportunities for device applications.

Black phosphorous is a bulk stable allotrope with phosphorous, a group-V element, covalently bonded in corrugated layers, with van der Waals forces holding the layers together. The recent investigations of phosphorene have sparked interest in analogous monolayered materials containing elements from the group IV and VI columns of the periodic table. Recently, nanometer-thin sheets of group IV-VI materials have been grown; these films are used in optoelectronics and photovoltaics [1]. However, there have been limited published success experimentally growing pure monolayer IV-VI samples [1,11]. Recent computational studies have explored the basic electronic properties of group IV-VI monolayers [12–14], although SiS monolayers were excluded from these initial studies. To date, exciton properties have not been calculated, even though excitonic effects are expected to dominate the optoelectronic properties of devices employing these materials [10].

Here we focus our attention on the excitonic effects for group-IV sulfur alloys: SiS, GeS, and SnS. Sulfur is a widely available source material. Devices employing these alloys would be environmentally benign and attractive for many applications. Thin films of GeS and SnS prefer the orthorhombic layered structure, analogous to black phosphorous [15–17]. While SiS is not thermodynamically stable in the layered orthorhombic structure, we find this structure to be metastable. Monolayered SiS has potential for integration into silicon-based electronics which would be of broad interest within the areas of nanoelectronics, optoelectronics, etc. Electronic energy bands for bulk and monolayer materials are calculated and compared with previous theory and experiment. All three monolayered materials have an indirect minimum electronic band gap. We report new computational predictions for the exciton binding energies in monolayer group-IV sulfur materials. In all three monolayer systems considered, although the minimum band gap is indirect, we predict a direct photoabsorption gap due to large excitonic effects. In GeS and SnS monolayers, two bound excitons are predicted and are due to nearly degenerate direct excitations. Overall, excitonic effects are expected to be critical to the photoresponse of these materials.

II. METHODOLOGY

To examine the properties of excitons in monolayer group-IV sulfur materials, we first begin with unit cells of the corresponding bulk orthorhombic crystals. With density functional calculations [18,19] we examine the properties of these sulfur materials using VASP [20,21]. A plane-wave basis with a cutoff energy of 300 eV was used. Standard projected augmented wave (PAW) potentials were used to treat core electrons [22,23]. Calculations were performed with the generalized-gradient corrected functional of Perdew, Becke,

and Ernzerhof (PBE) [24] to treat exchange and correlation. In addition, for bulk calculations, van der Waals (vdW) interactions were treated in a semiempirical fashion using the method of Grimme [25]. All atomic coordinates and lattice parameters were relaxed to their ($T = 0$ K) equilibrium values using a force tolerance of 0.01 eV/Å. For the initial bulk calculations, a $9 \times 7 \times 3$ k-point mesh was used for integrations over the Brillouin zone, whereas a denser k-point mesh is used for the subsequent band structure calculations.

Band-structure, effective-mass, and dielectric-function calculations were all performed at the PBE level. The static dielectric constants are determined in the independent particle approximation by diagonalizing the dielectric tensor as described in Ref. [26], where vibrational contributions have been excluded. For the bulk dielectric tensor, the three components are close and we report the average below. For the effective mass, we fit the energy near the band extrema to parabolas; sensitivity analysis indicates our uncertainty is $\sim 0.01\, m_e$.

To model a single monolayer in vacuum within the supercell approximation, we increase the perpendicular periodic lattice constant from its bulk value to create a vacuum layer of $L_{\text{vac}} \sim 20$ Å. This vacuum level is similar to the values used in previous work [13,27]. The size of the vacuum layer has a significant influence on the calculated value for the exciton properties and the dielectric constants. We estimate an overall uncertainty of 20% for the reported monolayer in-plane dielectric constants. Importantly, the out-of-plane dielectric constant is close to 1 as expected for a thin monolayer suspended in vacuum. The effect of vacuum layer size on physical properties is discussed in the Supplemental Material [28] under uncertainty analysis.

To understand exciton effects in monolayered materials, we need to go beyond the PBE level of theory. Therefore, we have calculated the quasiparticle, electronic structure using the non-self-consistent G_0W_0 approximation [29,30] which accounts for the many-body electron interactions but retains the input PBE wave functions. The G_0W_0 quasiparticle bands are calculated for $21 \times 21 \times 1$ k-point mesh. From the G_0W_0 quasiparticle bands, we calculate excitonic effects with the Bethe-Salpeter equation (BSE) which account for the interaction of a quasielectron and a quasihole. The present calculations employ the Tamm-Dancoff approximation as implemented in VASP [27]. The eight highest valence bands and the eight lowest conduction bands were used as a basis for excitonic eigenstates. Employing the BSE, we calculate direct band-to-band excitation energies and intensities which can be compared with optical absorption experiments.

A previous study [31] shows a clear dependence of exciton binding energy with k-point sampling, with errors of ~ 0.03 eV found in results employing coarser k-point grids. The extrapolation scheme introduced in Ref. [31] is beyond the scope of the present work. However, given our tests and previous work [14,31], we estimate an uncertainty of 0.1 eV for our exciton binding energy results. See the Supplemental Material [28] for more details regarding our test calculations.

The excitonic binding energy can be estimated using the semiclassical Mott-Wannier (MW) theory. In general, excitons extend in three-dimensional space. For thin films and monolayered materials, the in-plane and out-of-plane dielectric constants differ significantly. This leads to a complex Mott-Wannier problem that has been discussed previously in detail [32,33]. For monolayered materials there has been previous success approximating the excitons as being confined in two dimensions [29]. In the case of isotropic band masses, the two-dimensional MW binding energy (E_b) equation is

$$E_b = 4\frac{\mu_{\text{ex}} 13.6 \text{ eV}}{m_e \varepsilon^2}, \tag{1}$$

where ε is the planar dielectric constant and the exciton mass (μ_{ex}) is due to the conduction band electron and the valence band hole orbiting each other:

$$\mu_{\text{ex}} = \frac{m_e m_h}{m_e + m_h}. \tag{2}$$

Notice that in Eq. (1) the binding energy is inversely proportional to the dielectric constant squared so uncertainty in the static dielectric constant is amplified. In Sec. IV we compare our *ab initio* and semiclassical Mott-Wannier results.

III. RESULTS

We begin by examining the orthorhombic polymorphs of group-IV monosulfide bulk solids. The properties of bulk GeS and SnS are compared with experiment and previous theory. Then, the properties of the monolayered materials are calculated and, when possible, compared with previous theory. Two-particle excitation calculations with BSE reveal the presence of strongly bound excitons.

A. Bulk results

First, we consider the structural properties of orthorhombic bulk group-IV sulfide materials. We have relaxed the unit cell and internal coordinates using the PBE+vdW [25] method. The theoretical lattice constants are reported in Table S1 of the Supplemental Material [28]. No clear periodic trends are found in the lattice parameters. For GeS and SnS, calculated lattice constants are $\sim 2\%$ from their respective experimental lattice constants [16], as is typical of PBE calculations. SiS is thermodynamically stable as a periodic array of linear chains. However, the vibrational density of states calculated for the SiS layered polymorph is similar to that of GeS and SnS, indicating that SiS is metastable as a layered material (since there are no negative eigenfrequencies). Our vibrational results generally agree with previous PBE calculations for GeS and SnS [13].

The band structures of bulk GeS and SnS are well understood. The band edges are mainly due to hybridized p states [1,34]. The present PBE electronic energy bands along high symmetry directions are reported for SiS, GeS, and SnS in Fig. S2 of the Supplemental Material [28]. Our results are consistent with previous PBE studies for GeS and SnS [34]. We find the direct gap at Γ is 0.9 eV within PBE, close to the indirect minimum gap. Previously, the spin-orbit corrections were found to be inconsequential for GeS and have been omitted from the current work [21,34]. PBE band gap results are lower than the experimental photoconductivity gap [35], as expected. For SiS, the band structure deviates from that of GeS and SnS; the valence band maximum for SiS occurs between Γ and Z, whereas for SnS and GeS the maximum occurs between Γ and Y.

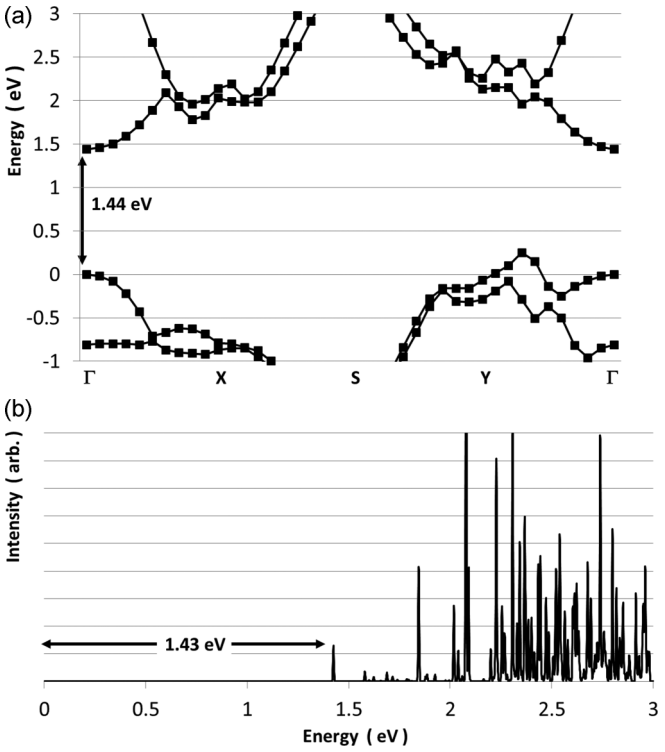

FIG. 1. (a) The G_0W_0 quasiparticle bands for bulk GeS are reported along with the lowest energy direct transition at Γ. The valence band maxima at Γ is set to zero energy. Only the states near the band edge are shown. (b) G_0W_0-BSE optical absorption intensity versus energy is reported for bulk GeS. The BSE absorption peak at 1.43 eV closely matches the G_0W_0 direct Γ excitation indicating a weakly bound exciton.

The static dielectric constants are calculated at the PBE level for bulk SiS, GeS, and SnS. For GeS, our results ($\varepsilon_{\text{ave}} \sim 11$) are close to both previous PBE results and the experimental values [4]. For SnS, our results ($\varepsilon_{\text{ave}} \sim 16$) are slightly higher than previous theoretical and experimental values [14]. The static dielectric constant for SiS ($\varepsilon_{\text{ave}} \sim 13$) is in between the GeS and SnS results. Because of the large dielectric constants of bulk group-IV sulfides, semiclassical Mott-Wannier exciton binding energies are small, less than 0.1 eV.

Optical absorption is mainly due to direct transitions. *Ab initio* exciton binding energies are calculated by taking the difference between G_0W_0-BSE optical absorption energies and the minimum direct G_0W_0 band gaps. In Fig. 1(a) we report G_0W_0 quasiparticle bands for bulk GeS (only the highest occupied and lowest unoccupied states are shown). The shape of the G_0W_0 bands closely follows the PBE results, justifying the previously used ad hoc scissor correction [34]. In Fig. 1(b) we show the G_0W_0-BSE optical absorption lines for GeS. The G_0W_0-BSE absorption energies are less than 0.1 eV from the respective direct G_0W_0 band transitions indicating that the *ab initio* exciton binding energies are less than 0.1 eV consistent with the Mott-Wannier estimate. As expected for large dielectric constant bulk materials, excitons are predicted to be only weakly bound. Excitons are examined in more detail for the monolayered materials below.

B. Monolayer results

The main objective is to provide predictions for the exciton binding energies for group-IV sulfide monolayers. First, the monolayers are structurally relaxed starting from a single layer of the bulk unit cell. In the direction perpendicular to the layer plane, the new supercell lattice is ∼2.0 nm to prevent any unwanted interactions between periodic images. We re-relax the coordinates. Then we calculate effective masses and dielectric constants at the PBE level of theory. At the G_0W_0 level of theory, we calculate the quasiparticle band structures and, at the G_0W_0-BSE level, we calculate the optical absorption energies and intensities.

All three systems considered have a similar monolayered band structure. Despite a topological difference in the bulk band structure of SiS, its monolayered band structure closely resembles that of GeS and SnS. All three materials have a valence-band maximum at a point between Y and $\Gamma(Y^* \sim 0.4\,Y)$, and a conduction-band minimum at $X^* \sim 0.4\,X$. Within the PBE method, the minimum indirect band gaps are 1.85, 2.17, and 1.83 eV for SiS, GeS, and SnS monolayers, respectively. The differences between the present work and previous calculations are small and can be attributed to the different computational approaches [12–14]. See Fig. S3 of the Supplemental Material [28] for the PBE band structure plots along high symmetry directions of the monolayered materials. The effective masses have been calculated for the main band extrema and are reported in Table S2 of the Supplemental Material. In general, the effective masses are found to be anisotropic with the $m(x) > m(y)$ for all materials considered. In addition, the effective masses at Γ are found to be larger than $1\,m_e$, whereas the other band masses are more typical of semiconductor materials with values ranging from 0.1 to $0.5\,m_e$. As expected, the static dielectric constants are lower than their bulk counterparts. The average static dielectric constants are 4.0, 3.9, and 4.7 for SiS, GeS, and SnS, respectively. The effective masses and dielectric constants are employed in the Mott-Wannier exciton binding energy calculations. See Table S3 for a full listing of MW binding energy results. Because of the larger effective masses at Γ, we find that the direct exciton binding energy at Γ is several tenths of an eV larger than the binding energy for excitons involving X^* or Y^*. In Table I we report the excitation and optical gaps along with the MW exciton binding energies for only the direct excitations at Γ.

The *ab initio* exciton binding energies are calculated using the G_0W_0-BSE method. We first calculate the G_0W_0 band structure for each monolayered material considered. Then the G_0W_0-BSE method is used to determine the two-particle excitations resulting in the optical absorption energies and intensities. Direct band excitations are expected to occur and the Mott-Wannier analysis indicates all three materials have a minimum absorption gap at Γ due to large excitonic effects.

Consider the G_0W_0 quasiparticle band structure for SiS reported in Fig. 2(a). The minimum direct band gap is 2.22 eV for a $\Gamma \rightarrow \Gamma$ excitation. The direct excitations are 3.17 eV for $X^* \rightarrow X^*$ and 2.97 eV for $Y^* \rightarrow Y^*$. The optical absorption intensity versus energy is reported in Fig. 2(b) for SiS. The minimum optical excitation occurs at 1.64 eV which is 0.58 eV lower than the minimum $\Gamma \rightarrow \Gamma$ G_0W_0 quasiparticle excitation, indicating a strongly bound exciton. This *ab initio* estimate for the exciton's binding energy matches

TABLE I. Monolayered materials' properties including average effective exciton mass (μ_{ex}), average dielectric constant (ε), G_0W_0 band gap at $\Gamma(\Gamma\ E_g)$, BSE optical band gaps (Opt. E_g), *ab initio* (BSE), and Mott-Wannier (MW) excitonic binding energies (E_b). Properties are calculated for the minimum direct gap at the Γ point. (See tables in Supplemental Material for further details on calculations.)

	$\mu_{ex}\,(x,\,y)\,(m_e)$	ε(none)	$G_0W_0\ \Gamma\ E_g$(eV)	BSE Opt. E_g(eV)	BSE E_b(eV)	MW E_b(eV)
SiS	0.92, 0.21	4.0	2.22	1.65	0.6	0.7
GeS	1.08, 0.43	3.9	2.69	2.03	0.7	1.2
SnS	0.90, 0.59	4.7	2.15	1.64	0.5	0.9

the Mott-Wannier estimate for the $\Gamma \rightarrow \Gamma$ point exciton, as reported in Table I. There is only one intense absorption peak below the G_0W_0 band edge indicating only one strongly bound exciton. This result is sensible since the $\Gamma \rightarrow \Gamma$ excitation energy is much smaller than the direct excitations at X^* and Y^*.

The predicted optical absorption spectra are a little more complex for GeS and SnS. Consider GeS, the G_0W_0 quasiparticle band structure is presented in Fig. 3(a). The direct G_0W_0 excitation at Γ is 2.67 eV; this value is close to the direct excitation at Y^* which is 2.63 eV. The direct excitation at X^* is much larger at 3.31 eV. The G_0W_0-BSE result for GeS is reported in Fig. 3(b). Two intense absorption peaks are found below the G_0W_0 band gap indicating that there are two strongly bound excitons. Our Mott-Wannier analysis indicates that the $\Gamma \rightarrow \Gamma$ exciton should have the largest binding energy since it has the largest effective mass. Comparing the lower G_0W_0–BSE peak with the $\Gamma \rightarrow \Gamma$ G_0W_0 excitation indicates the exciton's binding energy is 0.65 eV. Similar results are observed for SnS.

The G_0W_0 band structure for SnS is reported in Fig 4(a). Here the direct excitation at Γ is 2.15 eV, close to the value at X^* which is 2.28 eV. The optical absorption is calculated with the G_0W_0-BSE approach and reported in Fig. 4(b). Here the lowest optical peak is a low intensity peak but there are two more intense absorption peaks well below G_0W_0 band gap. These results indicate three strongly bound excitons exist for SnS monolayers. Only the most deeply bound excitons are recorded in Table I.

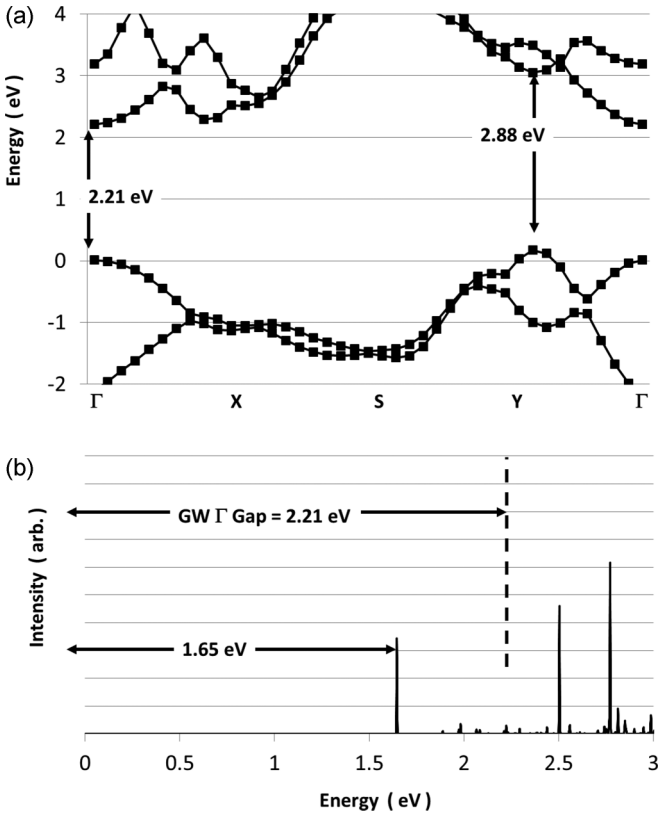

FIG. 2. (a) The G_0W_0 quasiparticle bands for monolayered SiS are reported along with the lowest energy direct transition at Γ. The valence band maxima at Γ is set to zero energy. Only the states near the band edge are shown. (b) G_0W_0-BSE optical absorption intensity versus energy is reported for monolayered SiS. The BSE absorption peak at 1.65 eV is well below the G_0W_0 direct Γ excitation indicating a strongly bound exciton.

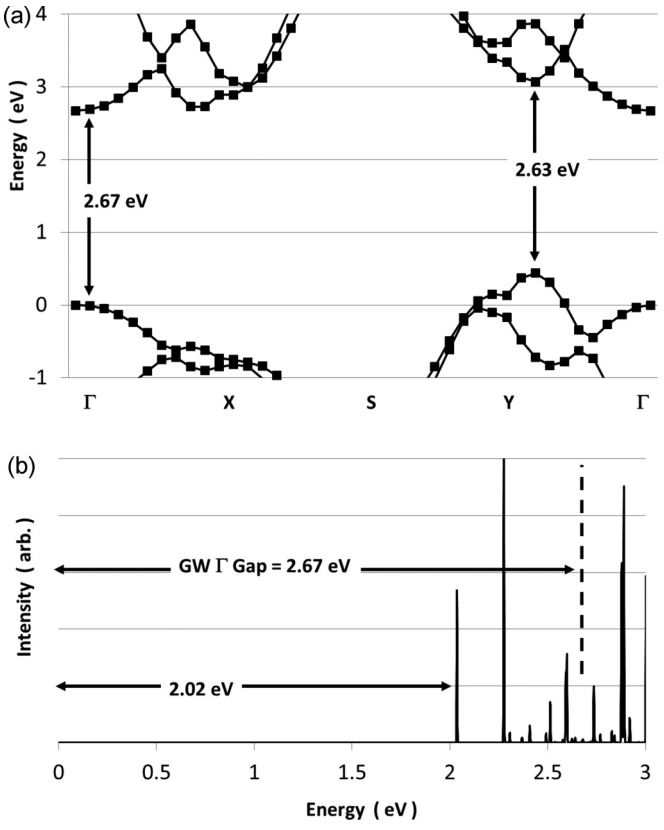

FIG. 3. (a) The G_0W_0 quasiparticle bands for monolayered GeS are reported along with the lowest energy direct transition at Γ. The valence band maxima at Γ is set to zero energy. Only the states near the band edge are shown. (b) G_0W_0-BSE optical absorption intensity versus energy is reported for monolayered GeS. The BSE absorption peak at 2.02 eV is well below the G_0W_0 direct Γ excitation indicating a strongly bound exciton.

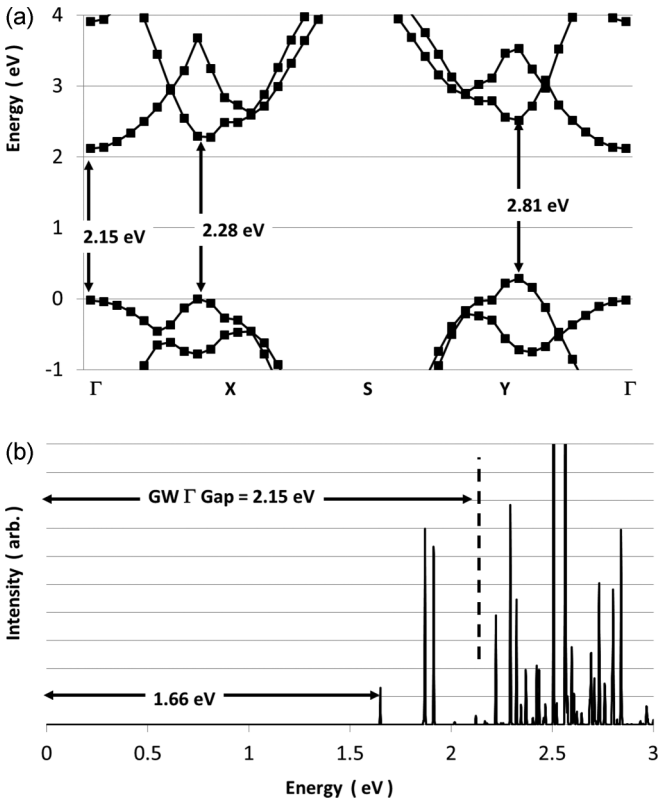

FIG. 4. (a) The G_0W_0 quasiparticle bands for monolayered SnS are reported along with the lowest energy direct transition at Γ. The valence band maxima at Γ is set to zero energy. Only the states near the band edge are shown. (b) G_0W_0-BSE optical absorption intensity versus energy is reported for monolayered SnS. The BSE absorption peak at 1.66 eV is well below the G_0W_0 direct Γ excitation indicating a strongly bound exciton.

IV. DISCUSSION

It is interesting to consider the present *ab initio* G_0W_0-BSE results in the context of the semiclassical Mott-Wannier (MW) theory. The Mott-Wannier Hamiltonian, which is hydrogenic, has been solved in two dimensions [36] in the case of isotropic band masses. The binding energy is presented in Eq. (1) above. Hydrogenic Hamiltonians have been solved in a number of circumstances including anisotropic masses [32,37]. The case here for anisotropic masses in two dimensions is described by the following Hamiltonian:

$$H = -\frac{\hbar^2}{2\mu_{\rm ex}^x}\frac{\partial^2}{\partial x^2} - \frac{\hbar^2}{2\mu_{\rm ex}^y}\frac{\partial^2}{\partial y^2} - \frac{e^2}{4\pi\varepsilon_o\varepsilon}\frac{1}{\sqrt{x^2+y^2}}, \quad (3)$$

which does not lend itself to an analytic solution. The exciton masses are defined for the x and y directions independently using Eq. (2) and the data from Table S2 in the Supplemental Material [28]. To find the ground state energy, we employ the variational method and the following elliptically symmetric wave function:

$$\psi = A\ \exp\left[-\sqrt{\left(\frac{x}{a}\right)^2 + \left(\frac{y}{b}\right)^2}\right], \quad (4)$$

where A is the normalization constant and the variational parameters are a and b which also define the ground state radii for the wave function. We solve for the binding energy using standard numerical methods. Our numerical result is identical to Eq. (1) in the case of isotropic band masses. In Table S3 we report our results for the Mott-Wannier binding energy (MW BE), effective exciton masses ($\mu_{\rm ex}$), and radii (a and b) for all band minima.

In Table I we summarize the results for the minimum energy excitations. For SiS monolayers, the Mott-Wannier result is close to the G_0W_0-BSE result. Such close agreement between G_0W_0-BSE and MW theory was also observed for metal dichalcogenides, which have deeply bound excitons from between 0.7 and 1 eV [8,27]. For GeS and SnS monolayers, the G_0W_0-BSE binding energy results are smaller than found from classical Mott-Wannier theory. Given the approximations and uncertainties involved, the present agreement between MW and BSE is reasonable.

When comparing the present theoretical results with future absorption and photoluminescence experiments, it is important to keep in mind that the present *ab initio* results are for direct excitations only. Because all three monolayered materials are indirect semiconductors, phonon-assisted absorption will be important at room temperature. Because the exciton binding energy is proportional to the effective band mass and the Γ band masses are much larger than other bands (see Table S2), the $\Gamma \rightarrow \Gamma$ exciton is predicted to be the most deeply bound exciton for these monolayered materials. The spectra due to less deeply bound excitons may include contributions from indirect excitons not considered here. The effect of these extra excitons may be to increase the intensity and/or broaden the observed secondary absorption peaks.

V. CONCLUSIONS

In summary, state-of-the-art many-body electronic structure calculations were combined to predict the direct exciton binding energies for group-IV sulfide monolayers SiS, GeS, and SnS. The presence of strongly bound excitons was found for all three monolayers. For SnS and GeS, multiple bound excitons were found with GeS excitons exhibiting the largest binding energy based on both the BSE and MW results. Experimental photoabsorption peaks are predicted to occur between 1.5 and 2 eV which suggests these monolayered materials will be useful for optical applications in the near infrared to red regime. The results here indicate that excitonic effects will be important when employing these monolayers in optoelectronic devices.

ACKNOWLEDGMENTS

This work was supported in part by the Gas Subcommittee Research and Development under Abu Dhabi National Oil Company (ADNOC) and by the McMinn Endowment at Vanderbilt University. Calculations were performed in part on the Penn State Lion X supercomputers.

[1] M. Xu, T. Liang, M. Shi, and H. Chen, Chem. Rev. **113**, 3766 (2013).
[2] S. Z. Butler, S. M. Hollen, L. Cao, Y. Cui, J. A. Gupta, H. R. Gutiérrez, T. F. Heinz, S. S. Hong, J. Huang, A. F. Ismach, E. Johnston-Halperin, M. Kuno, V. V. Plashnitsa, R. D. Robinson, R. S. Ruoff, S. Salahuddin, J. Shan, L. Shi, M. G. Spencer, M. Terrones, W. Windl, and J. E. Goldberger, ACS Nano **7**, 2898 (2013).
[3] A. K. Singh, K. Mathew, H. L. Zhuang, and R. G. Hennig, J. Phys. Chem. Lett. **6**, 1087 (2015).
[4] H. L. Zhuang, A. K. Singh, and R. G. Hennig, Phys. Rev. B **87**, 165415 (2013).
[5] H. Liu, A. T. Neal, Z. Zhu, Z. Luo, X. Xu, D. Tománek, and P. D. Ye, ACS Nano **8**, 4033 (2014).
[6] V. Tran, R. Soklaski, Y. Liang, and L. Yang, Phys. Rev. B **89**, 235319 (2014).
[7] A. Chernikov, T. C. Berkelbach, H. M. Hill, A. Rigosi, Y. Li, O. B. Aslan, D. R. Reichman, M. S. Hybertsen, and T. F. Heinz, Phys. Rev. Lett. **113**, 076802 (2014).
[8] H. J. Conley, B. Wang, J. I. Ziegler, R. F. Haglund, S. T. Pantelides, and K. I. Bolotin, Nano Lett. **13**, 3626 (2013).
[9] T. Cheiwchanchamnangij and W. R. Lambrecht, Phys. Rev. B **85**, 205302 (2012).
[10] R. S. Sundaram, M. Engel, A. Lombardo, R. Krupke, A. C. Ferrari, P. Avouris, and M. Steiner, Nano Lett. **13**, 1416 (2013).
[11] P. Sinsermsuksakul, J. Heo, W. Noh, A. S. Hock, and R. G. Gordon, Adv. Energy Mater. **1**, 1116 (2011).
[12] B. D. Malone and E. Kaxiras, Phys. Rev. B **87**, 245312 (2013).
[13] A. K. Singh and R. G. Hennig, Appl. Phys. Lett. **105**, 042103 (2014).
[14] G. A. Tritsaris, B. D. Malone, and E. Kaxiras, J. Appl. Phy. **113**, 233507 (2013).
[15] A. Okazaki, J. Phys. Soc. Jpn. **13**, 1151 (1958).
[16] H. Wiedemeier and H. G. von Schnering, Z. Kristallograph. **148**, 295 (1978).
[17] L.-M. Yu, A. Degiovanni, P. A. Thiry, J. Ghijsen, R. Caudano, and Ph. Lambin, Phys. Rev. B **47**, 16222 (1993).
[18] P. Hohenberg and W. Kohn, Phys. Rev. **136**, B864 (1964).
[19] W. Kohn and L. J. Sham, Phys. Rev. **140**, A1133 (1965).
[20] G. Kresse and J. Furthmüller, Phys. Rev. B **54**, 11169 (1996).
[21] G. Kresse and J. Furthmüller, Comput. Mater. Sci. **6**, 15 (1996).
[22] P. E. Blöchl, Phys. Rev. B **50**, 17953 (1994).
[23] G. Kresse and D. Joubert, Phys. Rev. B **59**, 1758 (1999).
[24] J. P. Perdew, K. Burke, and M. Ernzerhof, Phys. Rev. Lett. **77**, 3865 (1996).
[25] S. Grimme, J. Comp. Chem. **27**, 1787 (2006).
[26] M. Gajdoš, K. Hummer, G. Kresse, J. Furthmüller, and F. Bechstedt, Phys. Rev. B **73**, 045112 (2006).
[27] A. Ramasubramaniam, Phys. Rev. B **86**, 115409 (2012).
[28] See Supplemental Material at http://link.aps.org/supplemental/10.1103/PhysRevB.92.235405 for data from PBE and Mott Wannier calculations including uncertainty analysis.
[29] M. Shishkin and G. Kresse, Phys. Rev. B **74**, 035101 (2006).
[30] F. Fuchs, J. Furthmüller, F. Bechstedt, M. Shishkin, and G. Kresse, Phys. Rev. B **76**, 115109 (2007).
[31] F. Fuchs, C. Rödl, A. Schleife, and F. Bechstedt, Phys. Rev. B **78**, 085103 (2008).
[32] S. P. Andreev and T. V. Pavlova, Physica E **40**, 1551 (2008).
[33] L. V. Keldysh, JETP Lett. **29**, 716 (1979).
[34] L. Makinistian and E. A. Albanesi, Phys. Rev. B **74**, 045206 (2006).
[35] W. H. Strehlow and E. L. Cook, J. Phys. Chem. Ref. Data **2**, 163 (1973).
[36] X. L. Yang, S. H. Guo, F. T. Chan, K. W. Wong, and W. Y. Ching, Phys. Rev. A **43**, 1186 (1991).
[37] A. Schindlmayer, Eur. J. Phys. **18**, 374 (1997).